J. Phys. B: At. Mol. Opt. Phys. **42** (2009) 105204 (7pp) doi:10.1088/0953-4075/42/10/105204

R-matrix calculation of electron collisions with the BF^+ molecular ion

K Chakrabarti[1] **and Jonathan Tennyson**[2]

[1] Department of Mathematics, Scottish Church College, 1 & 3 Urquhart Sq, Kolkata 700006, India
[2] Department of Physics and Astronomy, University College London, Gower St, London WC1E 6BT, UK

Received 7 February 2009, in final form 7 April 2009
Published 8 May 2009
Online at stacks.iop.org/JPhysB/42/105204

Abstract
Electron collisions with the BF^+ molecular ion are studied using the framework of the diatomic version of the UK molecular *R*-matrix codes. A configuration-interaction calculation is performed for BF^+ to obtain potential energy curves and target properties for 14 lowest doublet and quartet states. Scattering calculations are performed which yield resonance parameters and excitation cross sections in the energy range 0–20 eV. Cross sections for rotational excitations and an approximate calculation for the electron impact dissociation cross section for BF^+ are also presented.

(Some figures in this article are in colour only in the electronic version)

1. Introduction

BF_3 plasmas are used in ion doping of silicon wafers for the manufacture of semiconductors. The principal ionic components of BF_3 plasmas are monatomic boron B^+ together with BF^+ and BF_2^+, BF^+ being the second most abundant ion species in such plasmas (Koo *et al* 2000). Ion doping techniques can use B^+, BF^+ or BF_2^+ or all of these as the dopant ions. Particularly if implants with monatomic boron ions are required, B^+ ions can be produced from the dissociation of BF^+ and BF_2^+ ions. In such cases, BF^+ can prove to be of a richer source of boron ions than BF_2^+ which contain only 33% boron. Though the BF^+ ion contents in such plasmas are low compared to BF_2^+, as shown in Koo *et al* (2000), the BF^+/BF_2^+ current ratio can be increased up to 50% in the accelerated ions, which in turn can enhance the boron ion yield. The present work was motivated by the importance of BF^+ in such processes.

Although considerable literature exists on the BF molecule (see Rosmus *et al* 1982, Schneider and Gianturco 1988, Bredohl *et al* 1988, da Costa *et al* 1992, Honingmann *et al* 1993, Mérawa *et al* 1997 and references therein), very little work on the BF^+ molecular ion has been reported. Rosmus *et al* (1982) calculated dipole moments and radiative transitions for the $^1\Sigma^+$ state of BF and the $^2\Sigma^+$ state of BF^+. In that work they also briefly studied the A $^2\Pi$ state of BF^+, which they found to be repulsive. Schneider and Gianturco (1988) obtained accurate potential energy curves for the X $^2\Sigma^+$ and A $^2\Pi$ states of BF^+ along with the X $^1\Sigma^+$ and A $^1\Pi$ states of BF over a wide range of internuclear distances.

However, to the best of our knowledge, cross sections for electron collisions with BF^+ have hitherto never been reported. In this paper, we consider electronic excitation and rotational excitation collisions between electrons and BF^+. In addition, we also present an approximate calculation of the cross sections for the electron impact dissociation of BF^+.

2. Calculations

2.1. Method

We use the *R*-matrix method. This divides the configuration space into two regions (Burke and Berrington 1993), an inner region defined by a sphere, here of radius 10 a_0, centred at the molecular centre of mass. This sphere encloses the entire *N*-electron target BF^+ wavefunction. In this inner region, the wavefunction of the $(N+1)$-electron system (BF^+ + electron) is given by

$$\Psi_k = \mathcal{A}\sum_{i,j} a_{i,j,k}\Phi_i(1,\ldots,N)F_{i,j}(N+1) + \sum_i b_{i,k}\chi_i(1,\ldots,N+1), \quad (1)$$

where $\mathcal{A}$ is the antisymmetrization operator, $F_{i,j}$ are continuum orbitals and χ_i are two-centre L^2 functions constructed from *N*-electron target orbitals. The L^2 functions allow for the

polarization of the N-electron target wavefunction in the presence of the projectile electron.

In equation (1), Φ_i is the wavefunction of the ith target state. Electron-correlation effects are included in these target wavefunctions via configuration interaction (CI) expansions. As discussed extensively in Tennyson (1996b), the choice of this CI expansion largely determines which L^2 functions are included in the wavefunction.

As BF^+ is a diatomic, we employ the diatomic version of the UK molecular R-matrix codes (Morgan *et al* 1998). This code uses Slater-type orbitals (STOs) to represent the target, and numerical orbitals in a partial wave expansion to represent the continuum (Tennyson and Morgan 1999). The approach necessitates the use of a Buttle (1967) correction to allow for the arbitrary fixed boundary conditions imposed on the continuum basis orbitals.

2.2. The BF^+ target

Whereas all previous calculations on BF^+ used Gaussian-type orbitals as basis functions, we have used the VB2 STOs of Ema *et al* (2003) which constitute six s-type, four p-type, two d-type and one f-type STOs centred on each atom. Test calculations with the STOs of Cade and Huo (1967) gave significantly worse results. The STOs of Ema *et al* were used to build a basis of 46 molecular orbitals containing 24σ, 14π, 6δ and 2ϕ orbitals. An initial SCF calculation was performed using these molecular orbitals for the lowest $^2\Sigma^+$ and $^2\Pi$ states of BF^+. The SCF molecular orbitals were then used in a CI calculation. In all calculations, the 1σ and 2σ orbitals were frozen. The CI calculations used the following configurations:

$(3\sigma, 4\sigma, 5\sigma, 1\pi)^9$,
$(3\sigma, 4\sigma, 5\sigma, 1\pi)^8\ (6\sigma - 24\sigma, 2\pi - 14\pi, 1\delta - 6\delta)^1$,
$(3\sigma, 4\sigma, 5\sigma, 1\pi)^7, (6\sigma - 24\sigma, 2\pi - 14\pi, 1\delta - 6\delta)^2$,

which correspond respectively to the complete active space (CAS) spanning valence orbitals, CAS plus single excitations out of the CAS and CAS plus double excitations.

Two sets of pseudo natural orbitals (NOs) were initially obtained by a CI calculation on the lowest $^2\Sigma^+$ and $^2\Pi$ states of BF^+. In the subsequent target state calculation, all σ orbitals and one π orbital in the target wavefunction were represented by $^2\Sigma^+$ NOs and the remaining π orbitals and all δ orbitals were represented by $^2\Pi$ NOs.

The excitation energies for the doublet and quartet states of BF^+ used in this work are summarized in table 1 for calculations performed at the BF equilibrium bond length of $R = 2.386\ a_0$. Our BF^+ model uses the NOs described above and a $(3\sigma,4\sigma,\ 5\sigma,\ 1\pi,\ 2\pi)^9$ CAS–CI wavefunction. The ground state and first excitation energies are compared to the very limited existing data: the calculations of Rosmus *et al* (1982) and of Schneider and Gianturco (1988). Our A $^2\Pi$ excitation energy is in reasonable agreement with the predictions of these two calculations. There appears to be no previous information on the other states tabulated.

Figure 1 shows the behaviour of the eight lowest doublet and quartet states of BF^+ used in our work as a function of the bond length. It can be seen that although some states show local minima, all excited states are predicted to be essentially

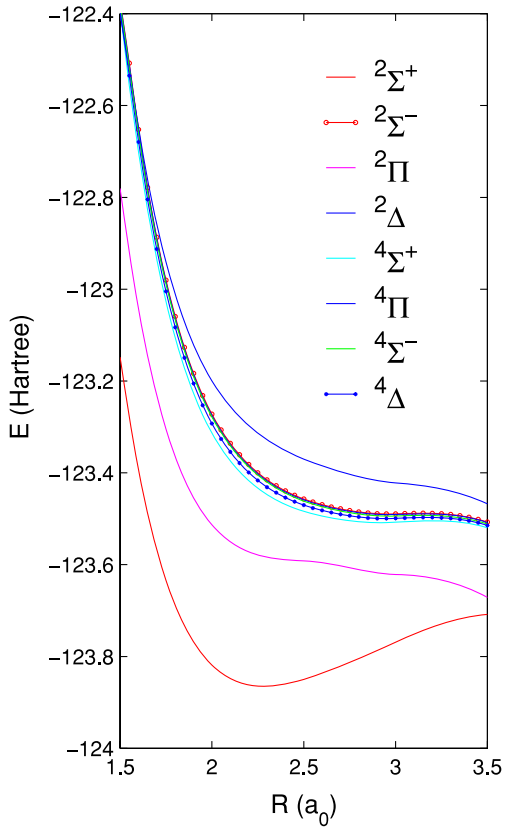

Figure 1. Potential energy curves for the eight lowest states of the BF^+ molecule.

Table 1. Ground-state energy (in Hartree) and vertical excitation energies (in eV) of the BF^+ molecule at $R_e = 2.386\ a_0$. $N(\Gamma)$ is the number of CSFs generated for each symmetry.

Excited state	Present	PNO/CEPA[a]	MRCD-I[b]
$N(^2\Sigma^+)$	**320**		
X $^2\Sigma^+$	−123.859 92	−124.083 75	−124.000 33
C $^2\Sigma^+$	11.14		
F $^2\Sigma^+$	13.64		
$N(^2\Sigma^-)$	264		
E $^2\Sigma^-$	11.52		
$N(^2\Pi)$	**486**		
A $^2\Pi$	7.38	7.6 ± 0.3	7.49
B $^2\Pi$	8.71		
$^2\Pi$	14.94		
$N(^2\Delta)$	**276**		
D $^2\Delta$	11.46		
H $^2\Delta$	16.52		
$N(^4\Sigma^+)$	**164**		
a $^4\Sigma^+$	10.70		
$N(^4\Sigma^-)$	**196**		
c $^4\Sigma^-$	11.39		
$N(^4\Pi)$	**292**		
d $^4\Pi$	13.90		
$N(^4\Delta)$	**152**		
b $^4\Delta$	11.12		

[a] From table 1 of Rosmus *et al* (1982).
[b] Interpolated form table 1 of Schneider and Gianturco (1988).

Table 2. The number and symmetry of target states used in the close-coupling expansion equation (1), as a function of total symmetry. The lowest energy target state of each symmetry was used in each case.

Symmetry	Number	Target states used
$^1\Sigma^+$	8	Three $^2\Sigma^+$ and $^2\Pi$ states plus two $^2\Delta$ states
$^1\Pi$	8	As above
$^1\Sigma^-$	6	One $^2\Sigma^-$ state, three $^2\Pi$ and two $^2\Delta$ states
$^1\Delta$	10	Three $^2\Sigma^+$, $^2\Sigma^-$, $^2\Pi$ states and one $^4\Delta$ state
$^3\Sigma^+$	11	Eight states as above plus one $^4\Sigma^+$, one $^4\Pi$ and one $^4\Delta$ state
$^3\Pi$	13	11 states as above plus one $^2\Sigma^-$ and one $^4\Sigma^-$ state
$^3\Sigma^-$	13	Three $^4\Sigma^-$ and $^2\Pi$ states, two $^4\Pi$ states, three $^2\Delta$ states and two $^4\Delta$ states
$^3\Delta$	14	Three $^2\Sigma^+$, $^2\Sigma^-$, $^2\Pi$, $^2\Delta$ states, one $^4\Sigma^+$ and one $^4\Delta$ state

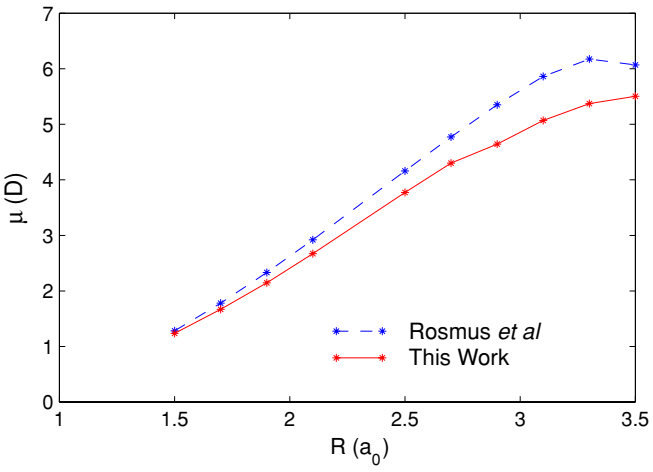

Figure 2. Dipole moments of the ground state of BF^+ as a function of bond length compared with the results of Rosmus *et al* (1982).

dissociative. Unfortunately the self-consistent field (SCF) procedure we used fails at bond lengths greater than 3.5 a_0 so this limited the range of our calculations.

BF^+ has a large dipole moment which has an important effect on the scattering cross sections, in particular those for rotational excitation, see below. Figure 2 presents the dipole moments of the ground state of BF^+ as a function of geometry. We compare our results with those of Rosmus *et al* (1982). The agreement of our results with their data is reasonable, though for larger bond lengths (beyond 2.8 a_0) our dipole is smaller by about 0.5 D.

2.3. The scattering model

We have used 14 ($8\sigma, 4\pi$ and 2δ) BF^+ natural orbitals in the scattering calculation. These were supplemented by continuum orbitals F_{ij} obtained as a truncated partial wave expansion around the centre of mass. Only partial waves with $l \leqslant 6$ and $m \leqslant 2$ were retained in the calculation. The radial parts of the continuum functions were generated as numerical solutions of an isotropic Coulomb potential. Those solutions with an energy below 10 Ryd were retained. This process produced 203 ($63\sigma, 52\pi, 42\delta$) continuum functions. To correct for linear dependence effects, we removed four σ continuum orbitals using Lagrange orthogonalization (Tennyson *et al* 1987); this number was selected by trial and error so that we deleted the minimum number of orbitals that gave stable results. The resulting set had $59\sigma, 52\pi$ and 42δ continuum orbitals which were then Schmidt orthogonalized to the target NOs.

Calculations were performed using the (3σ, 4σ, 5σ, $1\pi, 2\pi$)^9 CAS target wavefunction for the BF^+ states. Target orbitals not used in the CAS were treated in the same fashion as the continuum functions, $F_{i,j}$ in equation (1), and contracted with the target CI (Tennyson 1996a). Scattering calculations were performed for $^1\Sigma^+$, $^1\Sigma^-$, $^1\Pi$, $^1\Delta$, $^3\Sigma^+$, $^3\Sigma^-$, $^3\Pi$ and $^3\Delta$ total symmetries. The summary of different target states used for each symmetry in the close-coupling expansion of the electron wavefunction in equation (1) is presented in table 2. All calculations were performed within the standard adiabatic nuclei approximation (Chase 1956).

2.4. Results

In the following subsections, we present the data on resonances for singlet and triplet states and our results for electronic excitation, rotational excitation and electron impact dissociation, at the equilibrium bond length 2.386 a_0. To the best of our knowledge, there are no previous works in these areas and hence we do not have any data, experimental or theoretical, to compare any of these with.

2.4.1. Resonances. With the scattering formalism outlined above, the inner region solution described in equation (1) was used to construct an R-matrix at the boundary. In the outer region, the potential was given by the Coulomb potential together with the diagonal and off-diagonal dipole and quadrupole moments of the BF^+ target. The R-matrices were then propagated (Morgan 1984) in this potential till the wavefunction could be matched to asymptotic Coulomb functions (Barnett 1982) using the Gailitis expansion procedure of Noble and Nesbet (1984). Tests showed that propagating R-matrices to a distance 100 a_0 produced stable results and hence this value was used in all subsequent calculations. As is characteristic of electron collisions with molecular ions, the cross sections show many narrow resonances. These resonances were detected automatically and fitted to a Breit–Wigner form (Tennyson and Noble 1984). Tests showed that the resonance parameters are stable to the choice of initial energy grid. Tables 3 and 4 summarize our

Table 3. Resonance positions and widths (in Ryd) and effective quantum numbers, ν, at $R = 2.386\ a_0$ for singlet total symmetries of the BF molecule below the first two BF^+ excited states. Numbers within brackets indicate power of 10.

Below the A $^2\Pi$ state			Below the B $^2\Pi$ state		
Position	Width	ν	Position	Width	ν
$^1\Sigma^+$					
0.2119	0.2041(−01)	1.7344	0.5496	0.3346(−02)	3.3211
0.3497	0.3581(−01)	2.2668	0.5602	0.2939(−02)	3.5354
0.4047	0.7029(−02)	2.6759	0.5776	0.3271(−03)	3.9973
0.4440	0.4852(−03)	3.1565	0.5827	0.1430(−02)	4.1683
0.4649	0.4074(−02)	3.5480	0.5909	0.1271(−02)	4.5046
0.4816	0.6050(−03)	3.9933	0.6028	0.6751(−03)	5.1715
0.4883	0.6260(−03)	4.2239	0.6072	0.6658(−03)	5.4999
0.4996	0.7594(−03)	4.7275	0.6140	0.3788(−03)	6.1733
0.5039	0.1604(−03)	4.9751	0.6165	0.3947(−03)	6.4971
0.5045	0.2804(−04)	5.0078	0.6208	0.2352(−03)	7.1742
0.5075	0.1489(−03)	5.2140	0.6224	0.2543(−03)	7.4951
0.5135	0.5258(−03)	5.6926	0.6253	0.1585(−03)	8.1745
0.5162	0.1084(−03)	5.9664	0.6264	0.1733(−03)	8.4935
0.5167	0.1939(−04)	6.0113	0.6284	0.1102(−03)	9.1747
0.5184	0.7583(−04)	6.2145	0.6291	0.1236(−03)	9.4922
0.5219	0.3559(−03)	6.6796			
$^1\Pi$					
0.3094	0.5802(−02)	2.0632	0.5578	0.2294(−02)	3.4830
0.3631	0.1792(−01)	2.3487	0.5672	0.2171(−02)	3.7011
0.3823	0.6490(−02)	2.4840	0.5757	0.2881(−02)	3.9355
0.4049	0.2685(−02)	2.6779	0.5819	0.1696(−02)	4.1393
0.4239	0.1566(−02)	2.8812	0.5918	0.1092(−02)	4.5441
0.4351	0.3827(−03)	3.0263	0.5975	0.1810(−02)	4.8358
0.4445	0.2552(−02)	3.1653	0.6024	0.5908(−03)	5.1428
0.4619	0.3065(−02)	3.4838	0.6076	0.4944(−03)	5.5379
0.4723	0.7107(−03)	3.7262	0.6107	0.7982(−03)	5.8172
0.4788	0.5271(−03)	3.9056	0.6138	0.3234(−03)	6.1453
0.4810	0.2178(−03)	3.9740	0.6168	0.2850(−03)	6.5373
0.4821	0.3659(−03)	4.0112	0.6187	0.4572(−03)	6.8109
0.4839	0.1203(−03)	4.0667	0.6207	0.2016(−03)	7.1468
0.4893	0.1275(−03)	4.2619			
0.4948	0.1327(−03)	4.4940			
0.5013	0.4799(−03)	4.8223			
0.5035	0.4420(−04)	4.9462			
$^1\Delta$					
0.0565	0.7223(−01)	1.4318	0.5536	0.1768(−02)	3.3963
0.1962	0.1295(−01)	1.6950	0.5777	0.3918(−03)	3.9995
0.3901	0.3868(−02)	2.5463	0.5803	0.1380(−02)	4.0849
0.4383	0.1826(−02)	3.0709	0.5867	0.5325(−03)	4.3209
0.4720	0.2074(−02)	3.7186	0.6019	0.5075(−03)	5.1091
0.4807	0.2708(−03)	3.9656	0.6084	0.6701(−03)	5.6043
0.4870	0.2056(−03)	4.1750	0.6134	0.3422(−03)	6.1017
0.4964	0.7304(−03)	4.5691	0.6167	0.3493(−03)	6.5237
0.5035	0.1832(−03)	4.9498	0.6204	0.2170(−03)	7.1017
0.5044	0.1036(−04)	5.0046	0.6225	0.2098(−03)	7.5002
0.5068	0.1281(−03)	5.1645	0.6264	0.1380(−03)	8.4895
0.5118	0.3441(−03)	5.5530	0.6291	0.9636(−04)	9.4836
0.5160	0.1171(−03)	5.9386			
0.5180	0.7536(−04)	6.1610			
0.5210	0.1987(−03)	6.5443			
0.5235	0.8324(−03)	6.9257			

results for the singlet and triplet symmetries respectively for calculations performed at the BF^+ equilibrium separation.

Tables 3 and 4 also give the real part of the effective quantum number, ν; these were calculated using the energy difference between a resonance and the next excited state. Physically it is interesting to look at the quantum defect, $\mu = n - \nu$, where n is the principal quantum number. It is possible to identify several series characterized by (almost) constant μ; for example, the $^1\Sigma^+$ symmetry calculations show resonances with $\mu \approx 0.83$ for $n = 5$–10 and another series with $\mu \approx 0.50$ for $n = 4$–10. However the lowest $^1\Sigma^+$ resonance cannot be associated with either of these series and it is probable that this resonance is an intruder, i.e. one that should be associated with a higher lying electronic

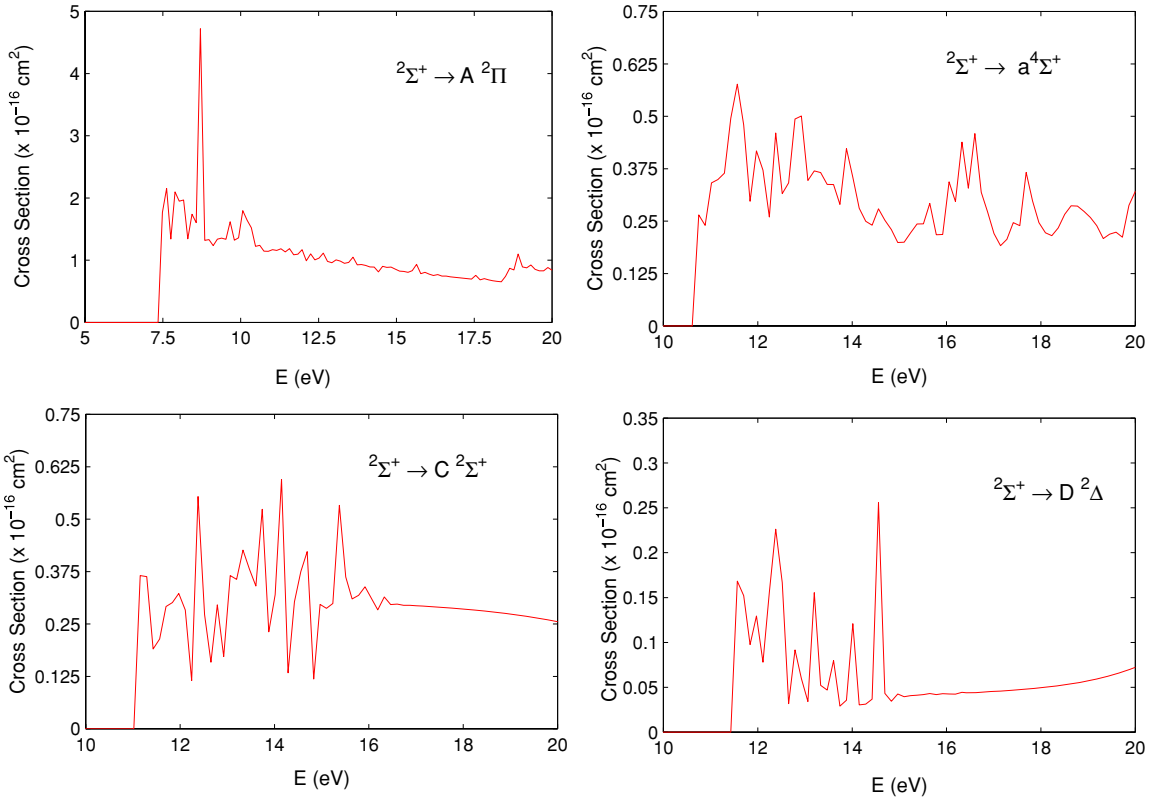

Figure 3. Excitation cross sections from the X $^2\Sigma^+$ ground state of the BF^+ molecule to the excited states indicated in each panel at $R = 2.386\ a_0$.

state. Given the close proximity of the two low-lying, $^2\Pi$ excited states and the presence of several other excited states at only slightly higher energies, several intruder states are to be anticipated. Identifying such intruders and linking the resonances with bound Rydberg states of BF is important for studies of dissociative recombination; work on this topic will be reported separately.

2.4.2. Electronic excitation and impact dissociation cross sections. Figure 3 shows cross sections for excitations from the ground state to the A $^2\Pi$, a $^4\Sigma^+$, C $^2\Sigma^+$ and D $^2\Delta$ excited states. In general, these electronic excitation cross sections are rather small, with only the lowest excitation, to the A $^2\Pi$ state, being significant. All the cross sections show a pronounced resonance structure. This is to be expected for fixed nuclei calculations on an ionic target; however, we do not expect that our calculation will reliably predict the precise positions of these resonance features as they are associated with higher lying electronic states whose positions are not particularly well represented in our target model.

Figure 4 presents our estimate of the electron impact dissociation of BF^+ at $R = 2.386\ a_0$. In calculating the electron impact dissociation, we assumed that all excitation to states above the BF^+ dissociation threshold of 4.99 eV (Rosmus *et al* 1982) result in dissociation. As indicated in our previous work (Chakrabarti and Tennyson 2007), the estimated cross section using this idea is not likely to be definitive. However this procedure gave a reasonable description of the experiment for the electron impact dissociation of CO^+ (Chakrabarti and Tennyson 2007). We expect this model to work even better for BF^+ where, as already noted, all the excited states are essentially dissociative. Again this cross section is fairly small, being little more than that the A $^2\Pi$ state excitation cross section shown in figure 4. This suggests that BF^+ should be fairly stable to electron impact dissociation.

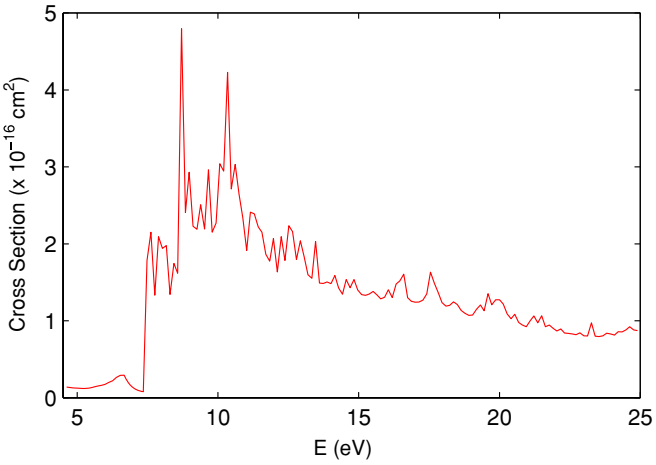

Figure 4. Estimated cross section for electron impact dissociation of the BF^+ molecule at $R = 2.386\ a_0$.

2.4.3. Rotational excitation. In diffuse media, the electron impact rotational excitation rate is crucial for determining the observable spectrum of the system (Lim *et al* 1999).

Table 4. Resonance positions and widths (in Ryd) and effective quantum numbers, ν, at $R = 2.386\ a_0$ for triplet total symmetries of the BF molecule below the first two BF^+ excited states. Numbers within brackets indicate power of 10.

Below the A $^2\Pi$ state			Below the B $^2\Pi$ state		
Position	Width	ν	Position	Width	ν
$^3\Sigma^+$					
0.0996	0.1665(−02)	1.4996	0.5444	0.2932(−03)	3.2311
0.3774	0.5805(−03)	2.4479	0.5561	0.2189(−02)	3.4473
0.4291	0.6264(−03)	2.9455	0.5777	0.3826(−03)	3.9991
0.4551	0.1098(−03)	3.3485	0.5886	0.1239(−02)	4.4018
0.4652	0.6926(−03)	3.5548	0.6058	0.6601(−03)	5.3923
0.4807	0.1805(−03)	3.9629	0.6157	0.3926(−03)	6.3829
0.4864	0.8041(−04)	4.1564	0.6218	0.2534(−03)	7.3707
0.4942	0.2286(−03)	4.4645	0.6246	0.9352(−04)	7.9967
0.5033	0.1189(−03)	4.9367	0.6259	0.1771(−03)	8.3534
0.5063	0.3995(−04)	5.1313	0.6287	0.1367(−03)	9.3278
0.5231	0.5929(−04)	6.8714			
$^3\Pi$					
0.2991	0.2230(−03)	2.0194	0.5527	0.3388(−02)	3.3800
0.3264	0.8333(−03)	2.1420	0.5670	0.1476(−02)	3.6957
0.3411	0.5691(−03)	2.2184	0.5715	0.2984(−02)	3.8133
0.3686	0.2061(−02)	2.3855	0.5778	0.3447(−03)	4.0013
0.3929	0.2515(−03)	2.5701	0.5820	0.1372(−02)	4.1455
0.4226	0.1101(−03)	2.8667	0.5918	0.1075(−02)	4.5424
0.4267	0.2805(−03)	2.9160	0.5963	0.7917(−03)	4.7694
0.4584	0.1441(−03)	3.4112	0.6024	0.6671(−03)	5.1399
0.4707	0.6680(−05)	3.6852	0.6063	0.4729(−03)	5.4246
0.4714	0.1375(−03)	3.7020	0.6077	0.6402(−03)	5.5470
0.4784	0.7767(−04)	3.8946	0.6101	0.3828(−03)	5.7639
0.4817	0.1857(−04)	3.9973	0.6137	0.3682(−03)	6.1432
0.4931	0.5600(−04)	4.4220	0.6167	0.3115(−03)	6.5248
			0.6184	0.2149(−03)	6.7609
$^3\Delta$					
0.1156	0.2223(−03)	1.5273	0.5547	0.2241(−03)	3.4189
0.2323	0.2736(−02)	1.7903	0.5692	0.3986(−04)	3.7513
0.2324	0.2704(−02)	1.7904			
0.5011	0.1844(−05)	4.8121			

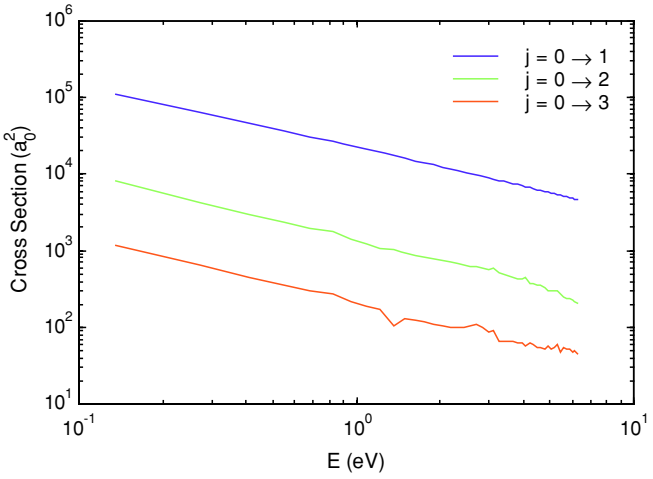

Figure 5. Rotational excitation cross sections of the BF^+ molecule at $R = 2.386\ a_0$ for excitations shown in the figure.

Figure 5 presents cross sections for the rotational excitations corresponding to the transitions $j = 0 \rightarrow 1$, $j = 0 \rightarrow 2$ and $j = 0 \rightarrow 3$. The geometry was frozen at BF^+ equilibrium bond length $R = 2.386\,a_0$ which gives a dipole moment of 3.4617 Debye. The cross sections were calculated using the ROTIONS program of Rabadán and Tennyson (1998). Excitation cross sections obtained from the T-matrix calculated above were supplemented by the dipole Coulomb–Born cross section (Chu and Dalgarno 1974) to include the contributions due to high-l partial waves. This procedure has recently been benchmarked against a much more complete approach and found to give excellent results even close to threshold (Faure *et al* 2006).

Excitations greater than $\Delta J = 3$ are negligible and therefore not considered. As has been found before for molecular ions with large dipole moments (Faure and Tennyson 2001), the rotational excitation cross section is dominated by $\Delta j = 1$ transitions at all energies.

3. Conclusion

To summarise, we have studied electron collisions with the BF^+ molecule using the molecular R-matrix method. Resonance parameters plus cross sections for electron impact electronic excitation and an estimate of the electron impact dissociation cross section are presented. We have also calculated the cross sections for rotational excitations

corresponding to transitions with $\Delta j = 1, 2$ and 3. This is the first information available for any of these processes.

References

Barnett A R 1982 *Comput. Phys. Commun.* **27** 147–66
Bredohl H, Dubois I and Mélen F 1988 *J. Mol. Spectrosc.* **129** 145–50
Burke P G and Berrington K A 1993 *Atomic and Molecular Processes—An R-matrix Approach* (Bristol: Institute of Physics Publishing)
Buttle P J A 1967 *Phys. Rev.* **160** 719–29
Cade P E and Huo W M 1967 *J. Chem. Phys.* **47** 614
Chakrabarti K and Tennyson J 2007 *J. Phys. B: At. Mol. Opt. Phys.* **40** 2135–45
Chase D M 1956 *Phys. Rev.* **104** 838–42
Chu S I and Dalgarno A 1974 *Phys. Rev.* **10** 788–92
da Costa H F M, Simas A M, Smith V H Jr and Trsic M 1992 *Chem. Phys. Lett.* **192** 195–98
Ema I, García De La Vega J M, Ramírez G, López R, Fernández Rico J, Meissner H and Paldus J 2003 *J. Comput. Chem.* **24** 859
Faure A and Tennyson J 2001 *Mon. Not. R. Astron. Soc.* **325** 443–8
Faure A, Kokoouline V, Green C H and Tennyson J 2006 *J. Phys. B: At. Mol. Opt. Phys.* **39** 4261–73
Honingmann M, Hirsch G and Buenker R J 1993 *Chem. Phys.* **172** 59–71
Huber K P and Herzberg G 1979 *Constants of Diatomic Molecules* (New York: Van Nostrand-Reinhold)
Koo B, Fang Z and Felch S 2000 *Proc. 13th Int. Conf. on Ion Implant Technology, IEEE* pp 504–7
Lim A J, Rabadán I and Tennyson J 1999 *Mon. Not. R. Astron. Soc.* **306** 473–8
Mérawa M, Bégué D, Rérat M and Pouchan C 1997 *Chem. Phys. Lett.* **280** 203–11
Morgan L A 1984 *Comput. Phys. Commun.* **31** 419–22
Morgan L A, Tennyson J and Gillan C J 1998 *Comput. Phys. Commun.* **114** 120–8
Noble C J and Nesbet R K 1984 *Comput. Phys. Commun.* **33** 399–411
Rabadán I and Tennyson J 1998 *Comput. Phys. Commun.* **114** 129–41
Rosmus P, Werner H J and Grim M 1982 *Chem. Phys. Lett.* **92** 250–6
Sarpal B K, Branchett S E, Tennyson J and Morgan L A 1991 *J. Phys. B: At. Mol. Opt. Phys.* **24** 3685–99
Schneider F and Gianturco F A 1988 *J. Phys. B: At. Mol. Opt. Phys.* **21** 329
Tennyson J 1996a *J. Phys. B: At. Mol. Opt. Phys.* **29** 1817–28
Tennyson J 1996b *J. Phys. B: At. Mol. Opt. Phys.* **29** 6185–201
Tennyson J and Morgan L A 1999 *Phil. Trans. R. Soc.* A **357** 1161–73
Tennyson J and Noble C J 1984 *Comput. Phys. Commun.* **33** 421–4
Tennyson J, Burke P G and Berrington K A 1987 *Comput. Phys. Commun.* **47** 207–12